Stimulated Raman spectroscopy and the determination of the *D*-fine-structure level separation in $^{40}Ca^{+}$

Rekishu Yamazaki
JST-CREST, 4-1-8 Honmachi, Kawaguchi, Saitama 331-0012, Japan

Hideyuki Sawamura
Graduate School of Engineering Science, Osaka University, 1-3 Machikaneyama, Toyonaka, Osaka 560-8531, Japan

Kenji Toyoda and Shinji Urabe
Graduate School of Engineering Science, Osaka University, 1-3 Machikaneyama, Toyonaka, Osaka 560-8531, Japan and JST-CREST, 4-1-8 Honmachi, Kawaguchi, Saitama 331-0012, Japan

(Received 8 August 2007; published 23 January 2008)

We describe the results of stimulated Raman spectroscopy between the fine-structure levels, specifically $3d^2D_{3/2}$ and $3d^2D_{5/2}$ metastable states, in a single trapped $^{40}Ca^{+}$. Transitions between different Zeeman sublevels, split by an applied magnetic field, are clearly observed and the fine-structure level separation of $\nu = 1\,819\,599\,021\,504 \pm 37$ Hz is determined. This measurement provides a direct observation of this level separation. From the spectroscopic data, a prospect of using the *D*-fine structure levels as a qubit for the quantum information processing is reviewed.

DOI: 10.1103/PhysRevA.77.012508 PACS number(s): 32.30.−r, 03.67.Lx

I. INTRODUCTION

A unique environment of ions confined in the pseudopotential well of the rf electric field trap has opened up a wide spectrum of physics in the past few decades. The confined ions can be cooled with a conventional laser cooling technique into the Lamb-Dicke regime, where the first order Doppler effect can be negligible, and can be quite isolated from the influence of the external environment [1]. The stable internal states of these isolated single ions can have very long coherence times and are therefore suited for the precision spectroscopy for tests of atomic theory [2], optical frequency standards [3], and quantum information processing [4,5].

Among all the ions used in the ion trap experiments, alkaline-earth ions, particularly Ca^{+}, Sr^{+}, and Ba^{+}, have a unique electronic characteristic of low-lying metastable *D*-fine structure levels. These *D*-metastable states with the *S*-ground state have been extensively used for the highly discriminative state detection in quantum information processing and for precision measurements. The use of these states can be extended for the metrology purpose as well. The *S*-*D* transition has been extensively studied for the single-ion optical frequency standard in alkaline-earth-like ions, including Hg^{+} [6], Sr^{+} [7], and Yb^{+} [8], and have demonstrated a fractional systematic frequency uncertainty of below 7.2×10^{-17} [6]. Champenois *et al.* recently proposed a frequency standard in the terahertz domain, using the *D*-fine structure levels. Unlike the other ion-trap frequency standards, the proposed frequency standard utilizes the trapped ion clouds to increase the clock signal and can achieve a stability of 8×10^{-14} at 1 s [9].

Despite the high demand and interest in the use of these states, very few studies have been performed to directly probe the level structures between the *D*-fine structure levels. The lack of study is largely because of the fact that these level separations range from 1.8 to 49 THz, which is a difficult range in which to obtain a narrow-line light source or a light modulator with such a high modulation bandwidth. Madej *et al.* measured the *D*-*D* transition in a barium ion driving a magnetic-dipole transition with a lead-salt diode laser [10]. The precision of the measurement was limited by a laser bandwidth of 40 MHz and the transition between different Zeeman sublevels was not resolved. They reported the fine-structure separation with an uncertainty of 11 MHz and a fractional uncertainty $\delta\nu/\nu = 4 \times 10^{-7}$. To the best of our knowledge, this is the only direct measurement between the *D*-fine structure levels in the alkaline-earth ions. Our current pursuit with calcium ions focuses on the development of a new qubit, using the energy level configuration, the $D_{3/2}$ and the $D_{5/2}$ metastable states (lifetime $\sim$1 s), briefly described in Ref. [11].

Relevant energy levels and the transition wavelengths of the calcium ion ($^{40}Ca^{+}$) are shown in Fig. 1. A significant advantage of the calcium ion for quantum information processing is that all the transitions shown in Fig. 1 can be accessed by commercially available diode lasers, important for future miniaturization of a quantum computer. A qubit using the $S_{1/2}$ ground and $D_{5/2}$ metastable states coupled via an electric quadrupole transition has been commonly used in the calcium ion [12], however, the weak coupling between the states could limit the gate speed. It is also necessary to build a stable laser, with the use of an ultrastable high finesse cavity, for robust information processing in this scheme. Our proposal for the *D*-state qubit includes the use of dipole-allowed Raman coupling between the metastable states to ensure a high gate speed and the use of phase-locked Raman lasers (850 and 854 nm in wavelength) to eliminate the need for an ultrastable high finesse cavity. As a part of the characterization of these prospective qubit levels, we perform a stimulated Raman spectroscopy between the Zeeman sublevels of the *D*-metastable states with a phase-locked laser system previously developed. We also determine the *D*-fine structure level separation using the spectroscopic data. We

 ©2008 The American Physical Society

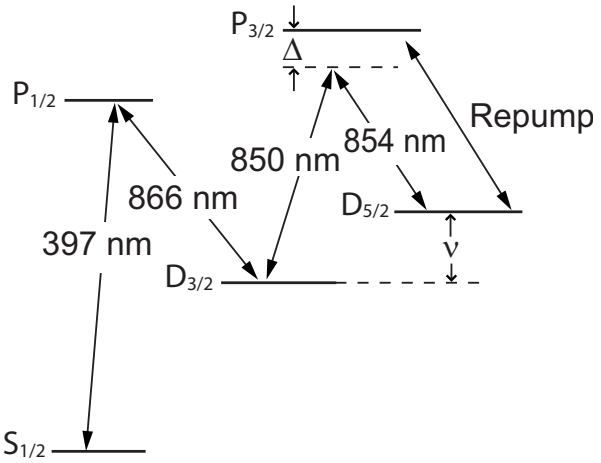

FIG. 1. An energy level diagram of the calcium ion showing the relevant transitions in the experiment. 397 and 866 nm lasers are used for the Doppler cooling of the ion. Raman transitions between $D_{3/2}$ and $D_{5/2}$ metastable state Zeeman sublevels are excited with phase-locked Raman lasers with wavelengths of 850 and 854 nm.

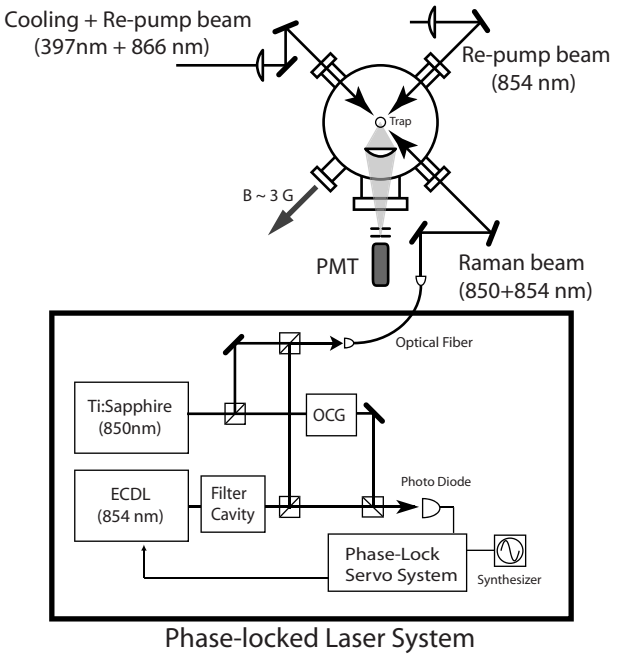

FIG. 2. The experimental setup. A single calcium ion, trapped with a spherical Paul trap inside the vacuum system, is cooled via Doppler cooling. The Raman beam is prepared from an output of Ti:sapphire laser (850 nm) and ECDL (854 nm), where two laser outputs are phase locked via the use of an optical comb generator (OCG) [11]. The Raman beam is sent to the ion trap with the beam propagation direction perpendicular to the quantization axis defined by the applied magnetic field. The transition by the Raman beam is measured from the observation of the uv fluorescence from the cooling cycle with a PMT.

show the experimental procedure in Sec. II, the results of the Raman spectroscopy and the determination of the D-fine structure level separation in Sec. III, and discuss the prospect of D-fine structure levels as a qubit in the Sec. IV.

II. EXPERIMENT

A schematic diagram of the experimental setup is shown in Fig. 2. A detailed explanation of the setup and the ion capturing and cooling method prior to the Raman spectroscopy is explained elsewhere [13] and we only discuss them briefly. We trap a single $^{40}Ca^{+}$ ion in a spherical Paul trap, consisting of a ring electrode, with an inner radius r_0 of 0.6 mm, and two end-cap electrodes. The electrodes of the trap are driven with voltage $V(t)=V_0\cos(\Omega t)$, with respect to the ring electrode, where $V_0=400$ V and $\Omega=(2\pi)$ 20 MHz are typically used. The neutral calcium gas is generated from a homemade oven, made of tungsten wire, inside the vacuum chamber and the ions are generated from the electron bombardment. The background pressure inside the vacuum system is 3×10^{-8} Pa. Four magnetic field coils are used to cancel the Earth's magnetic field and to define the quantization axis at the trap center. A typical magnetic field strength of 2–4 G is applied to define the quantization axis during the experiment. The uv fluorescence, 397 nm in wavelength, from the cooling cycle is measured with a photomultiplier tube (PMT). A cold-pass filter is used to reduce the infrared noise and apertures are placed in front of the PMT to eliminate unnecessary stray light from the trap.

The laser system used in the experiment consists of four external cavity diode lasers (ECDL) and a Ti:sapphire laser pumped with a second harmonic (532 nm) of a Nd:YAG laser. The output of two ECDLs, with corresponding wavelengths of 397 and 866 nm, are used for the Doppler cooling and repumping from the $D_{3/2}$ state, respectively. The output of another ECDL, 854 nm in wavelength, is used to repump the electrons from the $D_{5/2}$ state to the cooling cycle. These ECDLs are all locked to temperature-stabilized reference cavities during the experiment. The Raman beams, the output of a Ti:sapphire laser, and a ECDL with a tapered amplifier are phase locked with a use of an optical comb generator (OCG) and a phase-lock servo system [11]. A part of the 850 nm Ti:sapphire laser output is sent to the OCG, with a free spectral range $f_{\mathrm{OCG}}=6.252$ GHz, and we lock the 854 nm ECDL output to the comb element 291 comb lines away from the input frequency of the OCG. The relative frequency of the Raman beams is controlled with the rf signal, generated from a synthesizer, mixed to the phase-lock servo system. A typical synthesizer output frequency f_{synth} around 267 MHz is used during the experiment. The frequency difference between the Raman beam ν_{Raman} reads

$$\nu_{\mathrm{Raman}} = f_{\mathrm{OCG}} \times n + f_{\mathrm{synth}} = 6.252\ \mathrm{GHz} \times 291 + 267\ \mathrm{MHz} = 1\,819\,599\ \mathrm{MHz}. \quad (1)$$

The OCG and rf synthesizer are both synchronized to a GPS clock (Temex Epsilon Clock 2S-DO) during the experiment. The output of the ECDL with a tapered amplifier contains a broad background amplified spontaneous emission (ASE) and is filtered by a ring filter cavity with a free spectral range of 1 GHz and a finesse of 600.

The phase-locked Raman beams are sent through a polarization-maintaining fiber near the ion-trap chamber. A common fiber is used for the Raman pair to avoid an unnecessary phase shift between the Raman beams due to the fiber noise. It is also important to ensure a good spatial beam overlap by the use of a common fiber, since the systematic determination of the ac Stark shift relies on the precise knowledge of the relative intensity of the Raman beams at the ion. We chose the Raman beams to be collinear to each other with their propagation direction set perpendicular to the quantization axis defined by the applied magnetic field. The beam geometry was chosen to suppress the excitation of the ion motional states. The Raman beams are kept far detuned, $\Delta=50$ GHz, from the $P_{3/2}$ state during the experiment to avoid scattering from the excited state. In order to control the total power or the relative power of the Raman beams, we adjust the variable neutral density filter placed in each Raman beam. A typical total beam power used during the experiment ranges from 50 μW to 3 mW for the estimated beam radius of $w=60$ μm at the trap center.

The general sequence for the stimulated Raman spectroscopy is composed of five different steps. (i) The ion is Doppler cooled with 397 and 866 nm lasers. (ii) The state is prepared, where the electron is transferred to $D_{3/2}$ manifolds, by turning off the repump beam prior to turning off the cooling beam. (iii) The Raman beam (850 nm+854 nm) is turned on to excite the transition between the $D_{3/2}$-$D_{5/2}$ states. (iv) The state is determined by turning on the cooling cycle. Strong fluorescence from the cooling cycle can only be seen if the electron is in the $D_{3/2}$, otherwise the electron resides in the $D_{5/2}$ state. (v) The second repumper laser (854 nm) is turned on to transfer the residual population in $D_{5/2}$ state back to the cooling cycle. All the beam turn on/off's are controlled with the AOMs. While the Raman beams are turned on, all other lasers are turned off to avoid an unnecessary ac Stark shift of the fine-structure states. For the Raman spectroscopy, we repeat this sequence for 400–1000 times at each Raman frequency.

III. RESULTS

A. Raman spectroscopy on the $D_{3/2}$-$D_{5/2}$ transitions

In order to identify different transitions between the Zeeman sublevels of the fine-structure states, we performed a Raman spectroscopy with a wide scan range and different beam polarizations. Neglecting the second order Zeeman shift, there are 18 possible transitions, among which four pairs are degenerate in the transition frequency. All 14 spectral lines between the Zeeman sublevels are observed and identified. An example of the observed transitions with the laser polarization set to π polarization is shown in Fig. 3(a). Four peaks in the figure correspond to $|\frac{3}{2}m_J\rangle \rightarrow |\frac{5}{2}m_J\rangle$ (in $|J\ m_J\rangle$ basis) with $m_J=-\frac{3}{2}$, $-\frac{1}{2}$, $\frac{1}{2}$, and $\frac{3}{2}$ from the left peak to the right peak, respectively. The observed peaks are well resolved as shown. The location of the peaks is compared with the calculated values and corresponds well with the magnetic field strength $B=2.93$ G and the center frequency 1 819 599.03 MHz.

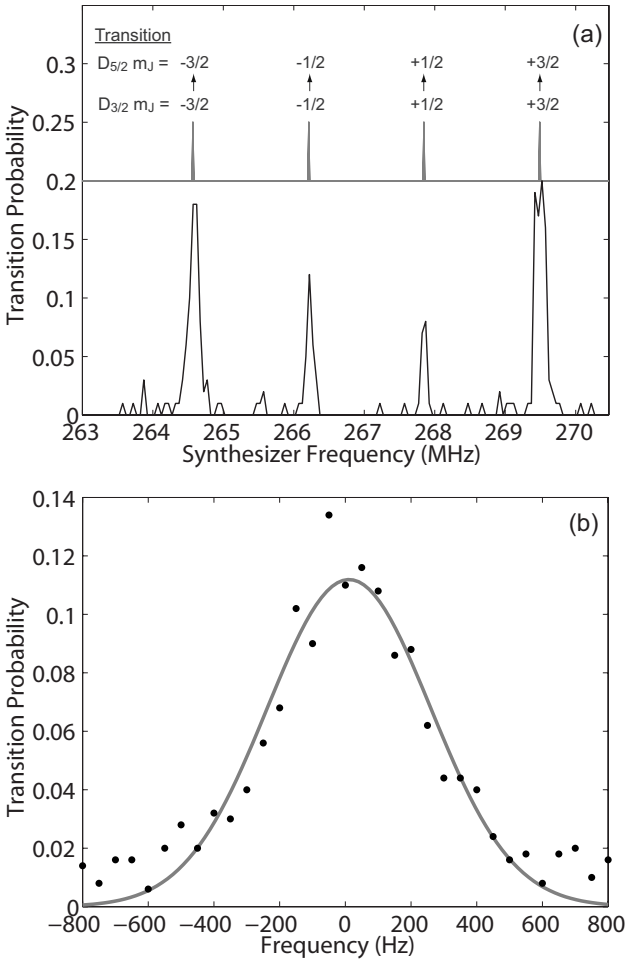

FIG. 3. Observed Raman spectra. (a) The transitions observed from the wide range scan. Spectra above the data show the calculated transition location for a magnetic field strength $B=2.96$ G and a center frequency 1 819 599.03 MHz. (b) Single spectra observed with a pulse duration of 5 ms. A narrow linewidth of approximately 470 Hz (FWHM) is observed.

In order to measure the systematic decoherence of these states, we perform a high-resolution scan of a single spectra, specifically on the $|J\ m_J\rangle:|\frac{3}{2}\frac{1}{2}\rangle \rightarrow |\frac{5}{2}\frac{1}{2}\rangle$ transition. Given a long interrogation pulse length and a low laser intensity of the probing laser, the phase-locked laser system can provide a very narrow transition linewidth. For the Zeeman levels with $m\neq 0$, the linewidth of the states is often dominated by the local magnetic field fluctuation and, therefore, this scan can provide an upper limit to the local magnetic field stability at the trap center. As shown in Fig. 3(b), a narrow linewidth of approximately 470 Hz [full width at half maximum (FWHM)] is observed for laser powers of 19.7 and 3.3 μW for 850 and 854 nm lasers, respectively, and a pulse duration of 5 ms. The observed spectra is much broader than the transient limited linewidth and the maximum residual magnetic field fluctuation of 0.8 mG is estimated at the trap center.

B. Determination of the fine-structure level separation

The level separation between the D-fine-structure levels ν can be determined by measuring the center of the symmetri-

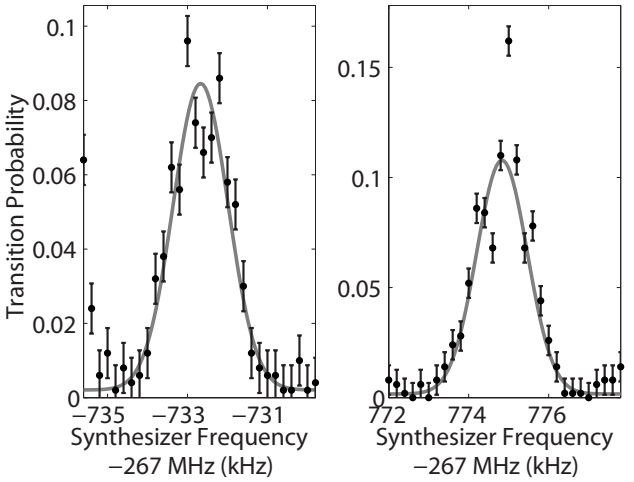

FIG. 4. Typical spectra observed for the transition $|J\ mJ\rangle$: $|_{52}-_{12}\rangle \rightarrow |_{32}-_{12}\rangle$ (left) and $|\frac{5}{2}\frac{1}{2}\rangle \rightarrow |\frac{3}{2}\frac{1}{2}\rangle$ (right). Two peaks are fitted with a Gaussian function to determine the peak center location. The center of two transitions ν is determined from the average of two peak locations.

cally distributed spectra due to the applied magnetic field. We perform a high-resolution spectroscopy of two middle peaks in the spectra, corresponding to $|J\ m_J\rangle$: $|\frac{5}{2}\frac{1}{2}\rangle \rightarrow |\frac{3}{2}\frac{1}{2}\rangle$ and $|\frac{5}{2}-\frac{1}{2}\rangle \rightarrow |\frac{3}{2}-\frac{1}{2}\rangle$ transitions, to determine the fine-structure level separation. The measurements are repeated with different total powers for the Raman beams and the power ratio between the two beams to account for the ac Stark shift.

For all the Zeeman sublevels probed during the measurement, the ac Stark shift from each Raman beam is expected to be linear in the laser power. The effect of the ac Stark shift on the level separation ν can be written in the form

$$\nu = \nu_0 + P_{854}A - P_{850}B \tag{2a}$$

$$= \nu_0 + \gamma P_{\text{total}}\left(A - B\frac{P_{850}}{P_{854}}\right). \tag{2b}$$

P_i and P_{total} are the power of the laser with a wavelength i and the total laser power, respectively. A and B are the shift constants for the 854 and 850 nm lasers, respectively. γ is the ratio of the 854 nm laser power to the total laser power ($\gamma = P_{854}/P_{\text{total}}$). ν_0 is the unshifted level separation that we seek.

A typical observation of two peaks and fitted curves are shown in Fig. 4. For each data set, we fit the observed peaks with a Gaussian function to determine the peak location, and the center of the peaks ν are calculated by taking the average of the two peak locations. From Eq. (2b), we expect the level separation between the D-fine structure to vary linearly with the total laser power while the power ratio between the Raman lasers is kept constant. In order to determine ν_0, we vary the total laser power to extrapolate ν at zero laser power. We repeated the measurement with several different power ratios between the Raman lasers, and examples of the measurements are shown in Fig. 5.

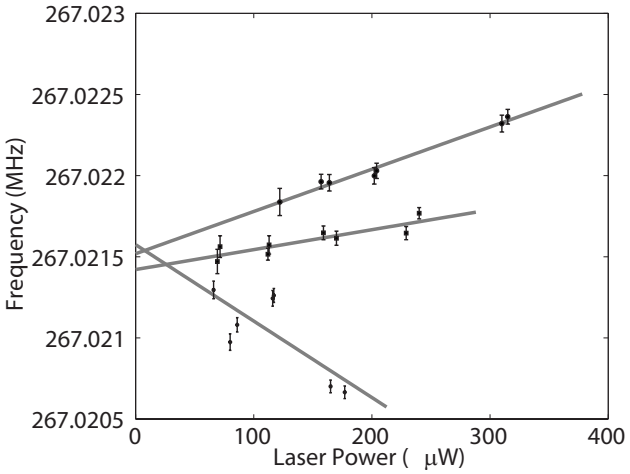

FIG. 5. Determination of the ac Stark shift and the fine-structure level separation. ν (without the OCG offset) determined from the average of the resonance frequencies of the transition $|J\ mJ\rangle$: $|_{52}-_{12}\rangle \rightarrow |_{32}-_{12}\rangle$ and $|\frac{5}{2}\frac{1}{2}\rangle \rightarrow |\frac{3}{2}\frac{1}{2}\rangle$ are plotted against the total Raman laser power. Lines in the figure show the line fit to the data measured with different power ratios between the Raman beams $P_{850}/P_{854}=33$, 23, and 5.5 from the top line to the bottom line, respectively.

The data collected with different Raman beam power ratios are each fitted with a straight line to determine the offset ν_0. When the power balance between the Raman beams is adjusted so that the ac Stark shift between the Zeeman levels of interest are equal, the slope of the line should approach zero. This corresponds to the vanishing condition of the second term in Eq. (2b). We experimentally determine the power ratio to be $P_{850}/P_{854}=20$ for the ac Stark shift balancing, similar to the calculated value of $P_{850}/P_{854}=21.3$.

The offset ν_0 obtained from seven trials with various Raman beam power ratios is shown in Fig. 6. From the data, we determined the fine-structure level separation of $\nu = 1\ 819\ 599\ 021\ 504$ Hz with a statistical uncertainty of 32

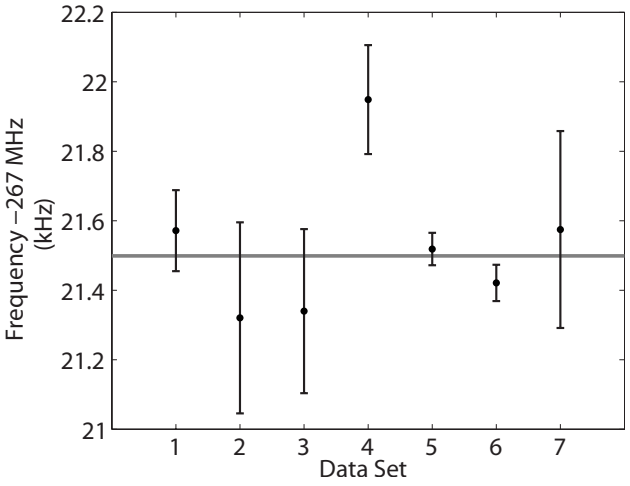

FIG. 6. Determination of the fine-structure level separation. ν (without the OCG offset) for seven different data sets is shown in the figure. We find a fine-structure level separation of $\nu = 1\ 819\ 599\ 021\ 504$ Hz $\pm$ 32 Hz.

Hz. The fractional uncertainty of the measured fine-structure level separation, $\delta\nu/\nu \simeq 32$ Hz/1.82 THz$=1.6\times10^{-11}$, is probably limited by the short term stability of our GPS clock system, 1×10^{-11} at 100 s.

In addition to the effect of the ac Stark shift by the Raman beams, the electric quadrupole shift is expected to be one of the largest sources of the level shift in most ion-trap experiments [14,15]. We minimize the electric field gradient in the trap by grounding the voltage applied to the end cap electrodes, with respect to the applied rf voltage $V(t)$, however, the effect of additional field gradient due to a patch potential is expected to be as large as $\frac{dE}{dz} \approx 4\times10^3$ V/cm^2. The estimated quadrupole shifts of the Zeeman sublevels $|m_J=\pm\frac{1}{2}\rangle$ of the $D_{3/2}$ and $D_{5/2}$ are 26.0 and 20.8 Hz, respectively, resulting in a 5.2 Hz uncertainty in the fine-structure level separation. Shifts due to other effects, including the Stark shift from the trap rf and the second order Zeeman shift, are all estimated to be below 0.1 Hz. We estimate the total uncertainty of the fine-structure level separation to be 37 Hz.

IV. $D_{3/2}$ AND $D_{5/2}$ METASTABLE STATES AS A PROSPECTIVE QUBIT

Criteria for a robust qubit includes a high fidelity for the gate operation and a long decoherence time (with respect to a gate time) of the qubit states. The measurements provided here support the use of D-fine structure levels as a qubit.

The observed transitions correspond to different Zeeman sublevels are all well resolved, indicating a highly selective transition to different sublevels. The error in a gate operation can originate from the fault transition to neighboring Zeeman sublevels, if the transitions were not well resolved. A long decoherence time of the qubit states can be expected from the measured linewidth, which can be as narrow as 470 Hz, in which the majority of the decoherence is expected from the magnetic field local fluctuation. With a proper magnetic field reduction, such as an active magnetic field cancellation or an installation of a magnetic field shield with a high permeability, the linewidth is expected to be reduced by at least an order of magnitude [16]. The gate speed is also expected to be high for this level scheme. During the Raman spectroscopy, we observed a power broadening of up to a few MHz for a moderate Raman laser output power of less than 1 mW. Current investigations include the measurement of a rapid Rabi oscillation between these levels.

The determination of the Raman beam power ratio to balance the level shift of the Zeeman sublevels of interest due to the ac Stark shift was performed for application in quantum information processing. It has been pointed out that the ac Stark effect induced from the strong laser field, necessary for fast gate operation, can shift the target energy level used for the manipulation. The resulting level shift can induce an extra phase factor to the gate operation, and has to be compensated. Häffner *et al.* reported a way of compensating the level shift by introducing an extra laser field, acting as a "antishifter" [17]. In the Raman configuration examined here, the same effect of level shift canceling can be achieved by controlling the relative power of the Raman lasers as shown. The ability to compensate for the level shift without introducing an extra laser field is another advantage of this configuration.

V. CONCLUSION

We performed stimulated Raman spectroscopy between the $D_{3/2}$ and $D_{5/2}$ metastable fine-structure levels in a single calcium ion. Well resolved transitions between different Zeeman sublevels are observed and a fine-structure level separation of $\nu=1\,819\,599\,021\,504$ Hz $\pm$ 37 Hz is determined. This study of the measurement of the D-fine structure level separation in an alkaline-earth ion reduced the fractional uncertainty of the level separation of Madej *et al.* by 10^{-4}. The transition has been proposed to be used as a terahertz metrology, and this study provides an important measurement for further investigations of the proposed scheme.

[1] D. J. Wineland, Science **226**, 395 (1984).
[2] N. Fortson, Phys. Rev. Lett. **70**, 2383 (1993).
[3] W. H. Oskay *et al.*, Phys. Rev. Lett. **97**, 020801 (2006).
[4] A. Steane, Appl. Phys. B: Lasers Opt. **64**, 623 (1997).
[5] C. Monroe, D. M. Meekhof, B. E. King, W. M. Itano, and D. J. Wineland, Phys. Rev. Lett. **75**, 4714 (1995).
[6] W. H. Oskay *et al.*, Phys. Rev. Lett. **97**, 020801 (2006).
[7] P. Dube, A. A. Madej, J. E. Bernard, L. Marmet, J. S. Boulanger, and S. Cundy, Phys. Rev. Lett. **95**, 033001 (2005).
[8] T. Schneider, E. Peik, and C. Tamm, Phys. Rev. Lett. **94**, 230801 (2005).
[9] C. Champenois, G. Hagel, M. Houssin, M. Knoop, C. Zumsteg, and F. Vedel, Phys. Rev. Lett. **99**, 013001 (2007).
[10] A. A. Madej, J. D. Sankey, G. R. Hanes, K. J. Siemsen, and A. R. W. McKellar, Phys. Rev. A **45**, 1742 (1992).
[11] R. Yamazaki, T. Iwai, K. Toyoda, and S. Urabe, Opt. Lett. **32**, 2085 (2007).
[12] *ARDA Quantum Information Science and Technology Roadmap*, http://qist.lanl.gov.
[13] H. Sawamura, H. Kitamura, K. Toyoda, and S. Urabe, Appl. Phys. B: Lasers Opt. **80**, 1011 (2005).
[14] W. H. Oskay, W. M. Itano, and J. C. Bergquist, Phys. Rev. Lett. **94**, 163001 (2005).
[15] C. F. Roos, M. Chwalla, K. Kim, M. Riebe, and R. Blatt, Nature (London) **443**, 316 (2006).
[16] T. W. Koerber, M. H. Schacht, K. R. G. Hendrickson, W. Nagourney, and E. N. Fortson, Phys. Rev. Lett. **88**, 143002 (2002).
[17] H. Haffner, S. Gulde, M. Riebe, G. Lancaster, C. Becher, J. Eschner, F. Schmidt-Kaler, and R. Blatt, Phys. Rev. Lett. **90**, 143602 (2003).